Photoactivatable Cross-Linked Polyacrylamide for the Site-Selective Immobilization of Antigens and Antibodies

Melanie S. Sanford, Paul T. Charles, Sarah M. Commisso, Jenna C. Roberts, and David W. Conrad*

Center for Biomolecular Science and Engineering, Code 6900, Naval Research Laboratory, Washington, D.C. 20375-5348

Received September 17, 1997. Revised Manuscript Received April 20, 1998

This paper describes the synthesis, characterization, and photochemical behavior of a new light-activated material for the photoimmobilization of antigens. The material is a derivative of cross-linked polyacrylamide that incorporates photoactive *o*-nitrobenzyl carbamates. When irradiated, the polymer undergoes a photochemical rearrangement to produce primary amines that can be used as molecular attachment sites. We monitored the photoconversion of thin (1−2 μm) polymer films that were deposited on silicon wafers or fused silica substrates using FT IR spectroscopy and UV−vis spectroscopy. To produce patterned polymer-modified substrates, we irradiated the material using a photolithographic mask. This process yielded 10-μm lines of photogenerated amines, to which an amine-reactive antigen (2,4,6-trintrobenzenesulfonic acid) was covalently bound. When we used this antigen-patterned substrate in a competitive fluorescence immunoassay containing tetramethylrhodamine-labeled anti-2,4-dinitrophenyl antibodies and 2,4-dinitrophenol, concentrations of 2,4-dinitrophenol as low as 2.3 μg/mL were detectable.

Introduction

Although conventional photolithography has provided many elegant methods for generating spatially resolved reactive surface functionalities,[1,2] many of these techniques are unsuitable for the immobilization of proteins due to their use of high-energy radiation, high temperatures, and denaturing organic solvents. Therefore, there is continuing interest in developing more biocompatible photoimmobilization techniques.[3−5] The ideal light-directed antibody immobilization scheme should (1) preserve the activity and optimize the orientation of the surface-bound antibody, (2) allow for control of site and surface density, and (3) provide sufficient resolution with minimal or well-characterized cross-reactivity between individual immobilization sites.

Various experimental approaches for the photopatterning of proteins onto solid supports have been reported. One early method used photooxidation of surface-bound organosilanes to produce discrete regions of differing hydrophobicity to which proteins were adsorbed or covalently attached.[6,7] Langmuir−Blodgett techniques and self-assembled monolayers (SAMs) have also been used to pattern proteins.[8−13] Direct photoimmobilization of proteins onto solid supports has been achieved using a variety of light-sensitive reagents[4] such as aryldiazirines,[14−16] aryl azides,[17−19] benzophenones,[16,20] and various *o*-nitro-protected functionalities.[21−23] The specific binding reaction between biotin and (strept)-avidin has been exploited to immobilize proteins through the use of various photoactivatable or photodeprotect-

* To whom correspondence should be addressed.

(1) *An Introduction to Microlithography: Theory, Materials, and Processing*; Thompson, L. F.; Wilson, C. G.; Bowden, M. J., Eds.; ACS Symposium Series 219; American Chemical Society: Washington, DC, 1983.
(2) Reiser, A. *Photoreactive Polymers: The Science and Technology of Resists*; John Wiley & Sons: New York, 1989.
(3) Fodor, S. P. A.; Read, J. L.; Pirrung, M. C.; Stryer, L.; Lu, A. T.; Solas, D. *Science* **1991**, *251*, 767.
(4) Sigrist, H.; Collioud, A.; Clémence, J. F.; Gao, H.; Luginbühl, R.; Sanger, M.; Sundarababu, G. *Opt. Eng.* **1995**, *34*, 2339.
(5) Connolly, P.; Moores, G. R.; Monaghan, W.; Shen, J.; Britland, S.; Clark, P. *Sens. Actuators B* **1992**, *6*, 113.
(6) Dulcey, C.; Georger, J.; Krauthamer, V.; Stenger, D.; Fare, T.; Calvert, J. *Science* **1991**, *252*, 551.
(7) Bhatia, S. K.; Teixeira, J. L.; Anderson, M.; Shriverlake, L. C.; Calvert, J. M.; Georger, J. H.; Hickman, J. J.; Dulcey, C. S.; Schoen, P. E.; Ligler, F. S. *Anal. Biochem.* **1993**, *208*, 197.
(8) Tender, L. M.; Worley, R. L.; Fan, H.; Lopez, G. P. *Langmuir* **1996**, *12*, 5515.
(9) Lopez, G. P.; Biebuyck, H. A.; Harter, R.; Kumar, A.; Whitesides, G. M. *J. Am. Chem. Soc.* **1993**, *115*, 10774.
(10) Singhvi, R.; Kumar, A.; Lopez, G.; Stephanopoulos, G.; Wang, D.; Whitesides, G.; Ingber, D. *Science* **1994**, *264*.
(11) Muller, W.; Ringsdorf, H.; Rump, E.; Wildburg, G.; Zhang, X.; Angermaier, L.; Knoll, W.; Liley, M.; Spinke, J. *Science* **1993**, *262*, 1706.
(12) Duschl, C.; Liley, M.; Corradin, G.; Vogel, H. *Biophys. J.* **1994**, *67*, 1229.
(13) Fang, J.; Knobler, C. M. *Langmuir* **1996**, *12*, 1368.
(14) Gao, H.; Sanger, M.; Luginbühl, R.; Sigrist, H. *Biosens. Bioelectron.* **1995**, *10*, 317.
(15) Collioud, A.; Clemence, J. F.; Sanger, M.; Sigrist, H. *Bioconjugate Chem.* **1993**, *4*, 528.
(16) Sundarababu, G.; Gao, H.; Sigrist, H. *Photochem. Photobiol.* **1995**, *61*, 540.
(17) Wybourne, M. N.; Wu, J. C.; Yan, M.; Cai, S. X.; Keana, J. F. W. *J. Vac. Sci. Technol. B*: **1993**, *11*, 2210.
(18) Yan, M.; Cai, S. X.; Wybourne, M. N.; Keana, J. F. W. *J. Am. Chem. Soc.* **1993**, *115*, 814.
(19) Matsuda, T.; Sugawara, T. *Langmuir* **1995**, *11*, 2267.
(20) Delamarche, E.; Sundarababu, G.; Biebuyck, H.; Michel, B.; Gerber, C.; Sigrist, H.; Wolf, H.; Ringsdorf, H.; Xanthopoulos, N.; Mathieu, H. J. *Langmuir* **1996**, *12*, 1997.
(21) Matsuda, T.; Sugawara, T. *Langmuir* **1995**, *11*, 2272.
(22) Holmes, C. P.; Solas, D. W.; Kiangsoontra, B. WIPO Patent Application WO 93-10162, 1993.
(23) Barrett, R. W.; Pirrung, M. C.; Stryer, L.; Holmes, C. P.; Sundberg, S. A. U.S. Patent 5,252,743, 1993.
(24) Pritchard, D. J.; Morgan, H.; Cooper, J. M. *Anal. Chem.* **1995**, *67*, 3605.
(25) Sundberg, S. A.; Barrett, R. A.; Pirrung, M.; Lu, A. L.; Kiangsoontra, B.; Holmes, C. P. *J. Am. Chem. Soc.* **1995**, *117*, 12050.

S0897-4756(97)00632-7 CCC: $15.00
Published on Web 05/30/1998

Scheme 1. Synthesis of *o*-Nitrobenzyl *N*-Allyl Carbamates

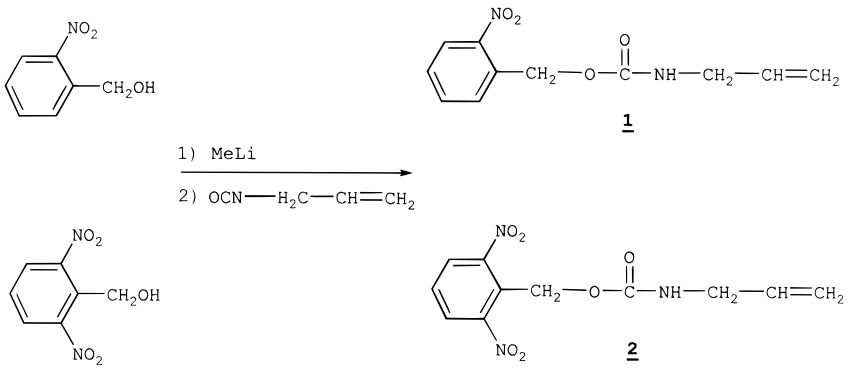

Scheme 2. Solution Photoconversion of 2,6-DNBAC with DUV Irradiation

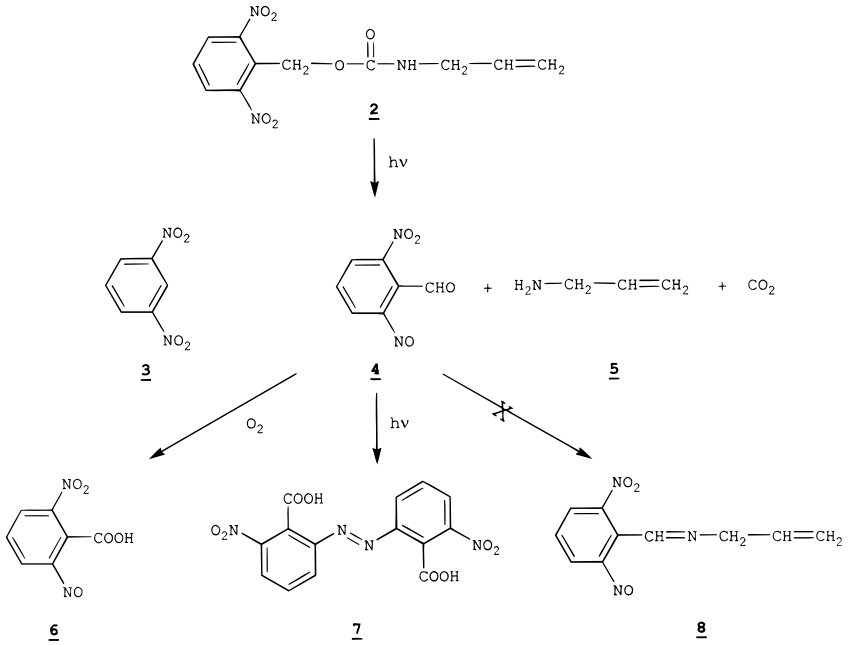

able derivatives of biotin.[24−29] Antibodies have also been covalently bound to aminated silica surfaces via poly(ethylene oxide) (PEO) spacers.[30] Recently, S layer proteins have been patterned on modified silicon surfaces using deep-UV (DUV) radiation.[31] Many of these methods require several surface modification steps to produce a substrate that is amenable to discrete protein immobilization.

In this paper, we report the preparation of a photoactive derivative of polyacrylamide which can be used for the site-specific immobilization of amine-reactive antigens without chemical pretreatment. We also introduce a new approach for patterning antibodies based on the prior light-directed immobilization of an antigen analogue. Finally, the antigen-patterned substrates are used in a competitive fluorescence immunoassay.

Results and Discussion

Synthesis of *o*-Nitrobenzyl *N*-Allyl Carbamates. We synthesized 2-nitrobenzyl *N*-allylcarbamate (2-NBAC) (**1**) and 2,6-dinitrobenzyl *N*-allylcarbamate (2,6-DNBAC) (**2**) to compare their photochemical efficiency for the production of primary amine groups in solution and in the solid state. Both were prepared by the one-step reaction of the corresponding nitrobenzyl alcohol with allyl isocyanate using a catalytic amount of methyllithium (Scheme 1).[32−35] While we were able to obtain pure **1** in 70% yield using extraction with hexane, flash chromatography (dichloromethane) was required for isolation of pure **2** in 62% yield.

Solution Photochemistry of Carbamates. Previously, it was shown for a similar series of carbamates that exposure to radiation below 340 nm caused an efficient photoinduced internal oxidation−reduction reaction to liberate amine, carbon dioxide, and an *o*-nitroso carbonyl byproduct.[36] Efficient photoconversions of **1** or **2**, however, required irradiation using DUV

(26) Hengsakul, M.; Cass, A. E. G. *Bioconjugate Chem.* **1996**, *7*, 249.
(27) Pritchard, D. J.; Morgan, H.; Cooper, J. M. *Angew. Chem., Int. Ed. Engl.* **1995**, *34*, 91.
(28) Koyano, T.; Saito, M.; Miyamoto, Y.; Kaifu, K.; Kato, M. *Biotechnol. Prog.* **1996**, *12*, 141.
(29) Pirrung, M. C.; Huang, C. Y. *Bioconjugate Chem.* **1996**, *7*, 317.
(30) Huang, S. C.; Caldwell, K. D.; Lin, J. N.; Wang, H. K.; Herron, J. N. *Langmuir* **1996**, *12*, 4292.
(31) Pum, D.; Stangl, G.; Sponer, C.; Fallman, W.; Sleytr, U. B. *Colloids Surf. B* **1997**, *8*, 157.
(32) Francis, P.; Thorne, N. P. *Can. J. Chem.* **1976**, *54*, 24.
(33) Cameron, J. F.; Fréchet, J. M. J. *J. Org. Chem.* **1990**, *55*, 5919.
(34) Fréchet, J. M. J.; Cameron, J. F. *J. Polym. Mater. Sci. Eng.* **1991**, *64*, 55.
(35) Cameron, J. F.; Fréchet, J. M. J. *J. Photochem. Photobiol. A: Chem.* **1991**, *59*, 105.

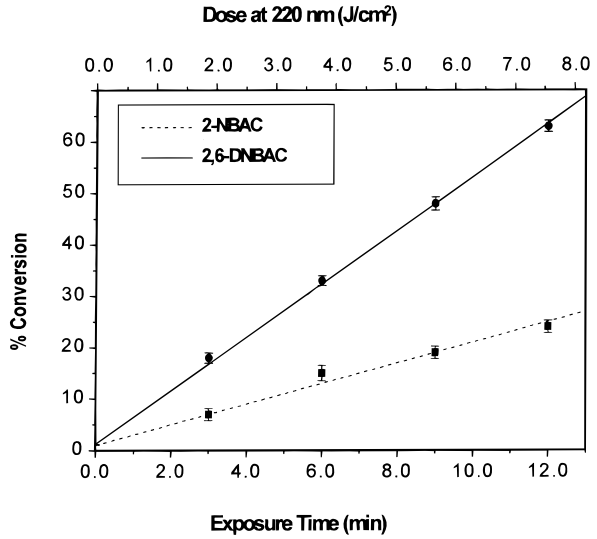

Figure 1. Solution-state photochemical conversion of **1** and **2** in acetonitrile as a function of exposure time and dosage. Error bars represent the standard deviations of the mean for $n = 3$.

light (220−260 nm, 10.5 mW cm^{-2} at 220 nm). Exposure at longer wavelengths led to very slow photoconversion due to substantial inner filter effects from secondary photoproducts (vide infra).

After irradiation of **2**, a singlet appeared at 10.5 ppm in the ^{1}H NMR spectrum for the carboxylic acid proton of 2-nitro-6-nitrosobenzoic acid (**6**) and at 1.2 ppm for the amine protons of allylamine (**5**) (See Scheme 2). Further evidence for the formation of primary amines was provided by a positive ninhydrin test. The percent conversions (determined from the chromatograms) versus exposure time/dose at 220 nm (10.5 mW cm^{-2}) for each carbamate are shown in Figure 1. At dose values greater than 9.45 J cm^{-2} (15 min, 25% conversion for **1**) the solutions turned yellow and the kinetic data became nonlinear due to internal filter effects. The faster rate of photo-rearrangement seen for the dinitro-substituted carbamate agrees with results obtained for a similar series of carbamates.[36]

To characterize the photoproducts of the more efficient reaction of **2**, the samples were subjected to thermal desorption chemical ionization mass spectrometry. The major products identified were **5** (*m*/*e* 57) and **6** (*m*/*e* 196).

Photolyses conducted with deoxygenated samples indicated that 2-nitro-6-nitrosobenzaldehyde (**4**) is easily oxidized to 2-nitro-6-nitrosobenzoic acid (**6**) unless the samples are thoroughly deoxygenated. Several other photoproducts were seen in the chromatograms due to secondary photochemistry of **4**. To identify these photobyproducts, thermospray/HPLC/MS was performed in both negative and positive ion modes. There were more ion peaks observed in negative mode for these nitro-substituted compounds. In positive mode, mostly ammonia adducts and ion clusters were detected. From the reconstructed ion chromatogram, we saw no evidence for the production of an imine adduct (**8**) (*m*/*e* 219)

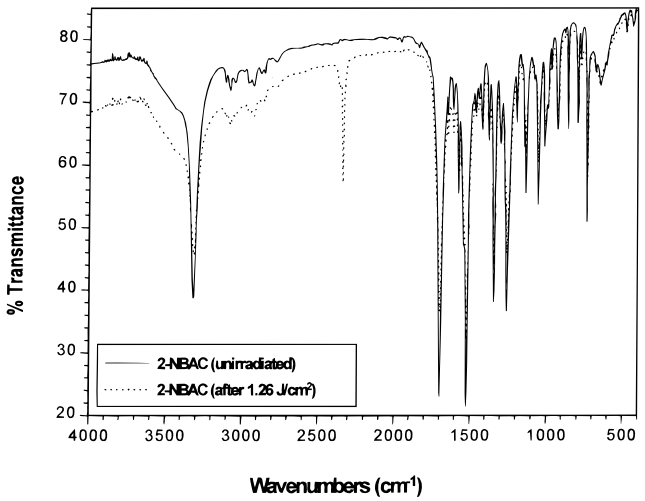

Figure 2. Infrared spectrum of **1** dispersed in KBr disk before and after irradiation.

as has been seen in the case of the *o*-nitrobenzyloxy carbonyl-protected amino acids.[38,39] One of the products formed in this system was 2-[(*E*)-2-(2-carboxy-3-nitrophenyl)-1-diazenyl]-6-nitrobenzoic acid (**7**) (*m*/*e* 360). Other workers had proposed similar adducts for the photolabile amino acid protective groups.[40] On the basis of the yellow color which develops during photolysis and the size of the peak in the chromatograms, we concluded that a substantial amount of **7** (which acts as an efficient internal light filter)[40,41] was generated. 1,3-Dinitrobenzene (**3**) (*m*/*e* 168) was also detected as a minor product. Small quantities (<5%) of this species were also detected during the isolation of **2** by flash chromatography.

Solid-State Photochemistry of Carbamates. We also followed the intramolecular photo-rearrangement of **1** and **2** in the solid state by monitoring changes in the N−H stretching frequency of the carbamate. When KBr pellets containing 0.24% (w/w) carbamate were exposed to DUV radiation, the N−H stretch at 3314 cm^{-1} for **1** and 3409 cm^{-1} for **2** decreased with increasing exposure dose. The observed change in the infrared spectrum on photolysis of **1** is shown in Figure 2.

The absence of broad N−H stretches (3300−3500 cm^{-1}) associated with **5** is conspicuous. Their absence may be due to the fact that the product is produced in the KBr matrix and is protonated by residual water to give the bromide salt, which would produce a broad peak around 3000 cm^{-1}. Analyses of the other spectral changes support the expected mode of photodecomposition outlined in Scheme 2. Irradiation causes a decrease in the intensity of the asymmetric N−O stretch (1530 cm^{-1}) and the symmetric N−O stretch (1342 cm^{-1}). The C═O band at 1697 cm^{-1} also decreases in intensity with the concomitant appearance of a strong band at 2338 cm^{-1} and a shoulder at 2361 cm^{-1}. This band combination is indicative of in situ generation of CO_2 which becomes trapped within the KBr matrix.[42]

(36) Cameron, J. F.; Fréchet, J. M. J. *J. Am. Chem. Soc.* **1991**, *113*, 4303.
(37) Huang M.; Vorkink, W. P.; Lee, M. L. *J. Microcolumn Sep.* **1992**, *4*, 233.
(38) Pillai, V. N. R. *Synthesis* **1980**, 1.
(39) Pillai, V. N. R. In *Organic Photochemistry*; Padwa, A., Ed.; Marcel Dekker: New York, 1987; p 225.
(40) Patchornik, A.; Amit, B.; Woodward, R. B. *J. Am. Chem. Soc.* **1970**, *92*, 6333.
(41) Ried, V. W.; Wilk, M. *Justus Liebigs Ann. Chem.* **1978**, *590*, 91.
(42) Pitts, J. N.; Wan, J. K. S.; Schuck, E. A. *J. Am. Chem. Soc.* **1964**, *86*, 3606.

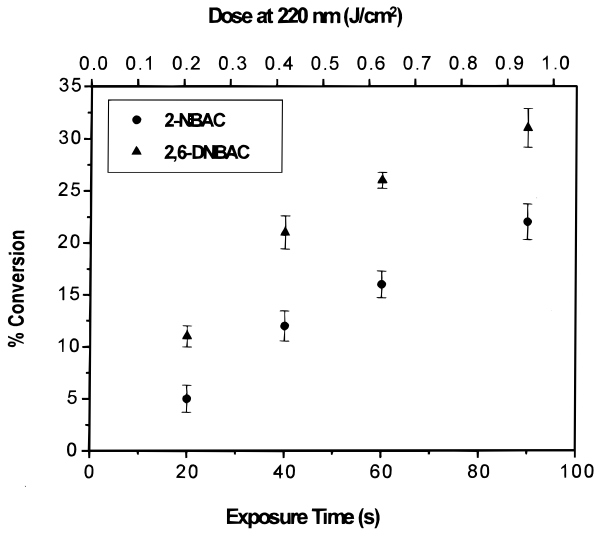

Figure 3. Solid-state photochemical conversion of **1** and **2** in KBr as a function of exposure time and dosage. Error bars represent the standard deviations of the mean for $n = 3$.

The percent conversion versus dose at 220 nm (10.5 mW cm^{-2}) for **1** and **2** is shown in Figure 3. At doses greater than 0.42 J cm^{-2} (40 s) the pellets turned yellow and the data became nonlinear due to inner filter effects (vide supra). As in solution, a faster rate of photorearrangement was observed for **2**. Moreover, the solid-state process for both **1** and **2** is approximately 6 times faster than the respective solution-phase process. To determine whether this increased rate of photo-decomposition was due to an alternate route leading to a different product distribution, the irradiated KBr disks were extracted with acetonitrile and analyzed by RPLC. The resulting chromatograms showed the presence of the same products, although there was less allylamine observed than in the solution case.

Polymerization of Photoactive Cross-Linked Polyacrylamide. The carbamates were synthesized with a vinyl group to allow for their participation in free radical polymerization reactions. The aim was to produce a polymer of acrylamide, *N*,*N*′-methylenebis-acrylamide (bis-acrylamide), and **1** or **2**. By incorporating a very small percentage of carbamate, it was hoped that the polymer could be made photoactive while retaining many of its desirable bulk properties (hydrophilicity, optical transparency) for antibody immobilization. During the polymerization reaction, the carbamate inserts into extending polymer chains to provide pendant mono- or dinitrobenzyloxycarbonyl-protected amine functionalities. These protecting groups can later be photo-deprotected and used as molecular attachment sites (Scheme 3).

The more water soluble and photochemically efficient 2,6-dinitrobenzyl *N*-allylcarbamate (**2**) was used in all polymerization studies. Initially, reactions were attempted in H_2O using 5% C and 40% T, where

$$\%T = \frac{\text{grams bis-acrylamide} + \text{grams acrylamide}}{\text{grams solvent}} \times 100 \quad (1)$$

$$\%C = \frac{\text{grams bis-acrylamide}}{\text{grams acrylamide} + \text{grams bis-acrylamide}} \times 100 \quad (2)$$

When **2** was incorporated into the mixture at 0.15% (w/w) and the reaction was performed using standard

Scheme 3. Photoconversion of 2,6-DNBAC-PA with DUV Irradiation

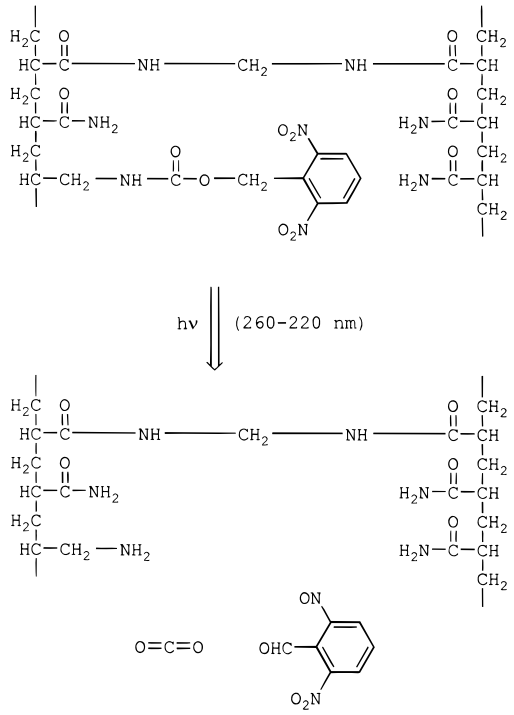

initiator and catalyst concentrations used for making polyacrylamide gels for electrophoresis,[43] no polymerization was observed even after 12 h at room temperature. This result was probably due to the previously observed inhibition of radical polymerization by nitroaromatics, although 4-nitrostyrene[44] and a copolymer containing *o*-nitrobenzyl acrylate[19] have been synthesized. Only after increasing the initiator (potassium persulfate) concentration from 0.05 to 0.4 mg/mL and the catalyst (TEMED) concentration from 0.01% to 0.3% (v/v) did polymerization occur. The kinetics of polymerization was investigated by monitoring the decrease in absorbance at 283 nm (due to a loss in UV-absorbing double bonds) as a function of time. In the present case, there was a 6-min induction period after which polymerization commenced. Although formation of a very rigid polymer was evident after 20 min at room temperature, the UV spectrum indicated that polymerization continued for an additional 70 min. While the polymer obtained under these conditions was nonelastic and transparent, it did exhibit a faint light brown color. This color probably indicates that there was some decomposition during polymerization. Nitroaromatics are known to be free radical scavengers,[45,46] and copolymers incorporating them frequently display some degree of brown color.[47] The amount of **2** that could be used in reactions was limited by its water solubility. Solutions were saturated at concentrations of 0.15% (w/w) at room temperature. When formamide was used as an

(43) Gelfi, C.; Righetti, P. G. *Electrophoresis* **1981**, *2*, 213.
(44) *Polymer Handbook*; Brandrup, J.; Immergut, E. H., Eds.; Wiley: New York, 1989.
(45) Foldes-Berezhnykh, T.; Szakacs, S.; Tudos, F. *Eur. Polym. J.* **1972**, *8*, 1237.
(46) Foldes-Berezhnykh, T.; Tudos, F.; Szakacs, S. *Eur. Polym. J.* **1972**, *8*, 1247.
(47) Hanson, J. E.; Reichmanis, E.; Houlihan, F. M.; Neenan, T. X. *Chem. Mater.* **1992**, *4*, 837.

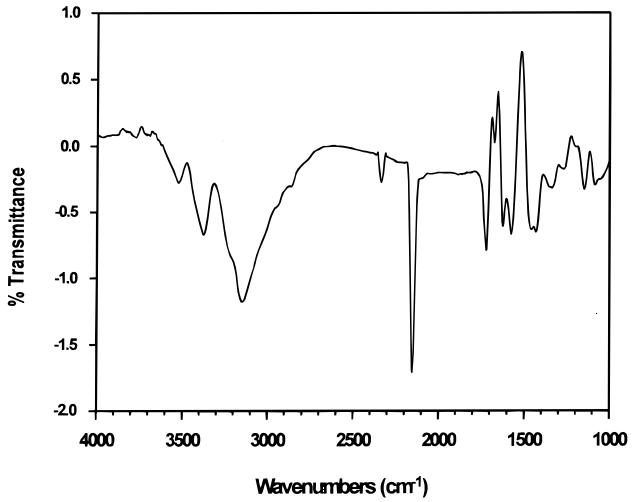

Figure 4. Infrared difference spectrum obtained after subtracting the spectrum of an unirradiated polyacrylamide film containing **2** from the spectrum obtained after irradiation (6.3 J/cm^{-2} at 220 nm).

alternative solvent, the solubility of **2** increased, but polymerization was incomplete, and cracked and opaque gels resulted. Although no attempt was made to measure the difference in reactivity between **2** and bisacrylamide during polymerization, we did try to extract any unreacted **2** from the resultant polymer using acetonitrile. The lack of any unreacted carbamate when the extract was subjected to HPLC suggests that **2** is fully incorporated into the polymer.

To use the polymer for the light-directed immobilization of antibodies for biosensor applications, it must be irreversibly bound to a solid substrate. We have used silicon wafers, fused silica slides, and microscope cover slips as polymer supports. We were able to covalently attach the polymer to the substrate by allowing the polymerization reaction to occur between two silane-modified substrates. Using the "flap technique",[48] we modified one substrate with 3-methacryloxypropyltrimethoxysilane (MPTS) and the other with dichlorodimethylsilane (See Experimental Section). After polymerization, the dichlorodimethylsilane-treated substrate was removed, leaving the polymer bound to the substrate containing vinyl groups donated by surface-bound MPTS. This technique produced well-anchored films as long as the polymer thickness was kept below 10 μm. Thicker films peeled away from the substrates when exposed to organic solvents or aqueous solutions of high ionic strength. Although we originally used 4-μm Mylar spacers between the substrates to control film thickness, we later discovered that reproducible films of 1−2-μm thickness could be produced using pressure plates instead of spacers.

Photo-Deprotection of Polyacrylamide Films. We used FT IR spectroscopy to study the photodeprotection of polyacrylamide films containing **2** (DNBAC−PA). The IR difference spectrum for DNBAC−PA (obtained by subtracting the spectrum of the unirradiated film from the spectrum obtained after a dose of 6.3 J cm^{-2} at 220 nm) is shown in Figure 4. Bands for the N−H stretch in photogenerated allylamine are observed at 3526 and 3379 cm^{-1}. The broad band at 3155 cm^{-1} may be due to the formation of the protonated amine salt. The in situ generation of carbon dioxide is evidenced by the stretch at 2339 cm^{-1}. The origin of the intense band at 2154 cm^{-1} is not well understood. This spectral feature was observed in irradiated samples prepared without the incorporation of **1** or **2** and may be due to the formation of CO from the polymer backbone in a reaction analogous to a Norrish type I process observed with ketones.[49] The stretch at 1724 cm^{-1} represents C═O arising from the production of aldehydes. Reduction of the nitro group is evidenced by the decrease in the intensity of the band at 1520 cm^{-1}.

The kinetics investigation of DNBAC−PA was conducted with the practical application of producing antibody-patterned substrates, as opposed to the more theoretical aim of investigating photoproducts and underlying reaction mechanisms. We were primarily interested in optimizing the reaction conditions and irradiation doses for the photochemical production of primary amines, which could later be used as antigen attachment sites. Direct determination of the extent of reaction in the polymer system proved to be difficult. The very small percentage of carbamate present in the polymer required the use of difference spectroscopy to probe changes induced by irradiation. This technique depends on the establishment of a reproducible background spectrum in the absence of photochemical conversion. Unfortunately, errors introduced by the inability to precisely reposition the sample in the spectrophotometer sample compartment after irradiation made this technique infeasible. To circumvent this problem, amines generated were detected as a function of exposure dose indirectly, using an amine-specific colorimetric reagent.

Fluorescamine is a nonfluorescent reagent that reacts with primary amines to form highly fluorescent compounds.[50] DNBAC−PA-coated fused silica slides were covered with metallized quartz line-space masks and irradiated for increasing time intervals. They were then reacted with a solution of fluorescamine. When the slides were examined under UV light (365 nm), green fluorescence emanated only from regions that were exposed. Fluorescence intensity continually increased for exposure times up to 30 minutes (18.9 J/cm^{-2} dose at 220 nm). At longer times, there was no increase in fluorescence, but the film surface continued to yellow. In control experiments, irradiated films of polyacrylamide without incorporated carbamate showed no fluorescence after reaction with fluorescamine.

We also used the reaction of 2,4,6-trinitrobenzenesulfonic acid (TNBSA) with primary amines to produce orange trinitrophenyl (TNP) derivatives[51,52] as a method of measuring the concentration of photogenerated amines in DNBAC−PA. When slides were irradiated for various time intervals and exposed to a solution of TNBSA, the polymer turned orange and the absorbance at 420 nm increased as a function of irradiation dose (Figure

(48) Radola, B. J. *Electrophoresis* **1980**, *1*, 43.

(49) Pitts, J. N., Jr.; Wan, J. K. S. In *The Chemistry of the Carbonyl Group*; Patia, S., Ed.; Wiley: New York, 1966; p 823.

(50) Udenfriend, S.; Stein, S.; Boehlen, P.; Dairman, W.; Leimgruber, W.; Weigele, M. *Science* **1972**, *178*, 871.

(51) Okuyama, T.; Satake, K. *J. Biochem. (Tokyo)* **1960**, *47*, 454.

(52) Inman, J. K. In *Methods in Enzymology;* Jakoby, W. B., Wilchek, M., Eds.; Academic: New York, 1974; Vol. 34, p 30.

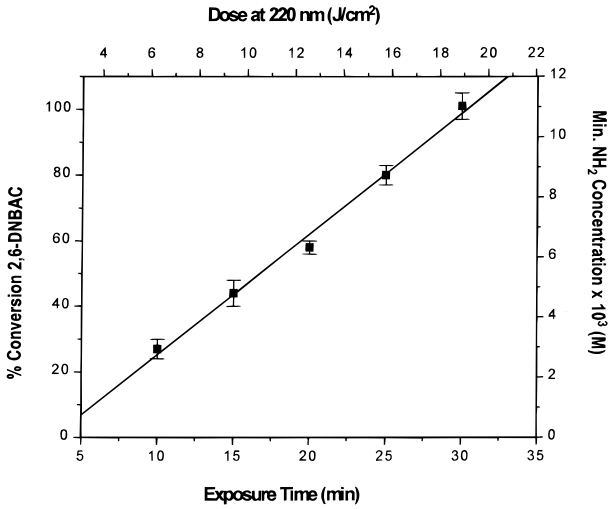

Figure 5. Photodeprotection of amines vs irradiation time and dose for DNBAC−PA. Amine concentration is based on a series of absorbance measurements made on films after a colorimetric reaction with TNBSA. Concentration values represent minimum amine concentrations based on 100% reaction yield. Error bars represent the standard deviations of the mean for $n = 3$.

5). Unirradiated films remained colorless when exposed to TNBSA and showed no increase in absorbance when examined by UV−vis spectroscopy. A limiting pore size of 19 nm was assumed for the cross-linked polyacrylamide composition used (5% C and 40% T). This assumption is based on a previous literature report in which polyacrylamide pore size as a function of %C and %T was determined from Ferguson plots of linear DNA fragments.[53] A small molecule such as TNBSA would be expected to freely diffuse throughout such a polymer matrix. After determining the polymer thickness, Beer's law was used to calculate the concentration of TNP amino groups and hence the concentration of free amines (assuming 100% reaction yield). At an irradiation dose of 19 J/cm^{-2}, the photogenerated amine concentration is equal to the original carbamate concentration and the photolysis is judged complete. The low percentage of **2** that is widely distributed along the polymer backbone may explain the linearity of the data due to the difficulty in forming **7**. Figure 5 also shows how the density of subsequently immobilized biomolecules can be controlled by varying the irradiation dose and, hence, the number of reactive surface functionalities.

Fluorescence Microscopy of Antigen/Antibody-Patterned Substrates. To produce an antigen/antibody-patterned substrate, we irradiated a DNBAC−PA-modified substrate (fused silica) through a line-space mask and then reacted it with TNBSA. The slide was then exposed to a solution of α-DNP-TRITC-IgG (10 μg/mL in PBS) for 30 min at room temperature. After rinsing with PBS and water, the substrate was air-dried and imaged. The resulting fluorescence micrograph is shown in Figure 6. The darker regions in the image correspond to areas of the polymer that were blocked from irradiation by the metal lines of the mask. In these areas, no photo-deprotection of amines has occurred, and hence there is no reaction with TNBSA. The

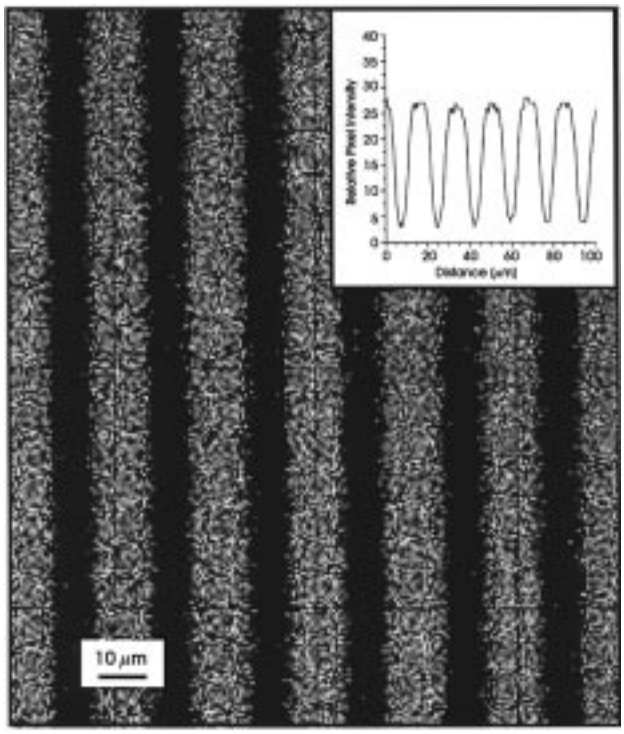

Figure 6. Fluorescence (excitation, 514 nm; emission, >565 nm) micrograph of TRITC-labeled α-DNP−IgGs bound to photopatterned trinitrophenyl (TNP) groups. The inset shows a graph of relative pixel intensity vs distance (plotted from left to right across the image).

lighter areas correspond to regions in which fluorescently labeled α-DNP antibodies are bound to trinitrophenyl groups. The inset shows a graph of relative pixel intensity for a square region (100 × 100 μm) extending from left to right across the image. The fluorescence contrast ratio of bright regions to dark regions is approximately 9:1. Control experiments, in which films were irradiated without subsequent reaction with TNBSA, produced no patterns when exposed to fluorescently labeled α-DNP antibodies prior to fluorescence imaging.

Antigen and Antibody Surface Concentrations. A summary of the results of antigen and antibody surface concentrations is presented in Table 1. The first row shows the incorporation of 2,6-DNBAC into cross-linked polyacrylamide, where the product concentration in this case is simply the initial amount of 2,6-DNBAC incorporated into the polymerizing solution. The second row of the table gives the concentration of TNBSA for samples irradiated for 30 min [(1.1 ± 0.05) × 10^{-2} M] and was obtained using UV−vis spectroscopy as described above. Nonspecific uptake in this case is a measure of the amount of TNBSA which is bound to the unirradiated polymer. This concentration was below the minimum detectable concentration (MDC). The surface concentration of ^{125}I-labeled antibodies bound specifically to patterned TNP-containing regions [(1.1 ± 0.4) × 10^{-11} mol/cm^2] assumes a nonporous polymer surface with no surface roughness. In actuality, the polymer surface may more closely resemble a cellular[54] or spongelike closed-cell structure.[55] The extent to

(53) Holmes, D. L.; Stellwagen, N. C. *Electrophoresis* **1991**, *12*, 612.

(54) Rüchel, R. *J. Chromatogr.* **1978**, *166*, 563.
(55) Rüchel, R. *Anal. Biochem.* **1975**, 415.

Table 1

Reaction	Product	Product Concentration	Nonspecific Uptake
acrylamide + *N,N*-methylenebisacrylamide + 2,6-DNBAC	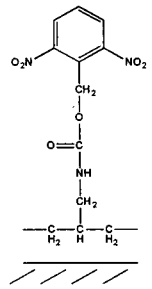	1.1 x 10^{-2} M 2,6-dinitrobenzyl N-allylcarbamate	NA
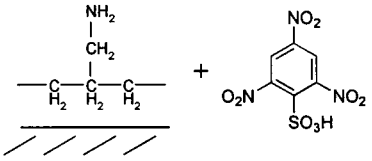	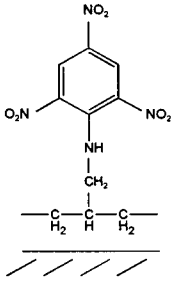	[a] (1.1 ± 0.05) x 10^{-2} M mean ± std. dev. (n = 3)	ND
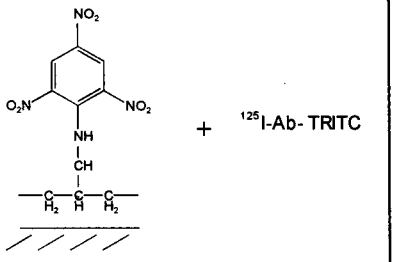	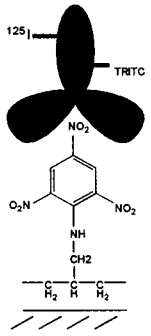	[b] (1.1 ± 0.4) x 10^{-11} (mol/cm^2) mean ± std. dev. (n = 3)	[b,c] (1.7 ± 0.3) x 10^{-12} (mol/cm^2) mean ± std. dev. (n = 3)

[a] Represents minimum concentration (see Results and Discussion). [b] Values are for a nonporous polymer surface with no surface roughness. [c] Surface concentration of ab bound nonspecifically to 2,6-DNBAC-PA in the absence of irradiation and subsequent reaction with TNBSA. NA = not applicable. ND = below the minimal detectable concentration.

which antibodies are able to penetrate into the film is also an important issue. When solutions of fluorescently labeled antibodies were exposed to thick (0.5 cm) sections of the polymer for 1 h and examined in cross section or by vertical scans along the *z*-axis with a LSCFM, fluorescence was observed to come only from the outermost regions of the film. On the basis of these results, it was concluded that antibodies are confined to the polymer surface. This result may be due to the aforementioned discussion of polymer porosity or to the fact that the time period may be too short to allow for full diffusive equilibrium. The nonspecific uptake of ^{125}I-labeled antibodies [(1.7 ± 0.3) × 10^{-12} mol/cm^2] is a measure of the amount of antibody bound to 2,6-DNBAC−PA in the absence of irradiation and subsequent reaction of TNBSA. Although the ratio of specific to nonspecific binding was lower than expected (8:1), the experiment was performed in the absence of any protein blocking agents (e.g., bovine serum albumin or casein) and included only a brief rinse with detergent and water (see Experimental Section). There was also no image correction (dark current or background subtraction) for intrinsic background fluorescence or light scattering from the polymer-coated substrate itself. Figure 6 is simply a raw image data file which is not enhanced in contrast and brightness. The fact that the fluorescence contrast ratio data agrees so well with the specific:nonspecific binding results of the ^{125}I-labeling experiments (9:1) (Table 1) supports the conclusion that these corrections would be minor in the present case.

Competition Immunoassay. We performed a competition immunoassay to determine if the patterned polymer substrates could be used to measure an unknown solution concentration of the antigen 2,4-DNP. In this assay format, 2,4-DNP and polymer-bound TNP compete for antibody binding sites. Solutions of α-DNP-TRITC-IgG (10 μg/mL in PBS) were fortified with 2,4-DNP to produce final antigen concentrations ranging from 0 to 50 μg/mL. These antigen/antibody solutions were applied to 2,6-DOCA−PA substrates and incubated for 30 min before being thoroughly rinsed with PBS, PBS/Triton X-405 [(1 × 10^4):1] and water. After drying the substrates in air, we examined them using fluorescence microscopy. The resulting fluorescence

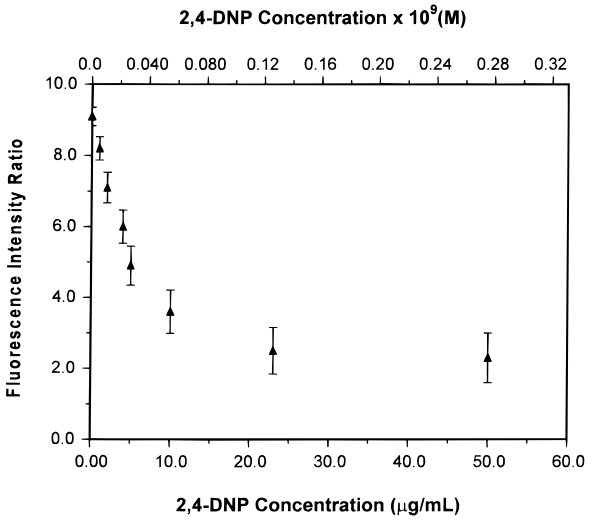

Figure 7. Competition immunoassay for the detection of 2,4-DNP. Solutions of α-DNP-TRITC-IgG (10 μg/mL in PBS) containing varying amounts of 2,4-DNP were exposed to TNP-patterned substrates, and the fluorescence intensity ratio was plotted versus 2,4-DNP concentration. Error bars represent the standard deviations of the mean for $n = 3$.

intensity ratios (bright regions:dark regions) for a series of antigen concentrations are shown in Figure 7. The use of fluorescence ratios (as opposed to average pixel intensity for the bright regions) helped alleviate errors introduced by variance in polymer layer thickness among individual substrates. As the concentration of 2,4-DNP is increased, the concentration of the antigen/antibody (2,4-DNP/α-DNP-TRITC-IgG) complex rises. These complexes are highly inefficient at binding to TNP sites on the polymer surface. Hence, 2,4-DNP competes with surface-bound TNP for antigen binding sites on the IgG. For a given concentration of α-DNP-TRITC-IgG, the amount of nonspecific binding to unirradiated regions of the polymer determines the dynamic range over which concentrations can be determined. In the present system, the fluorescence ratio in the absence of any added 2,4-DNP is 9.0. At concentrations above 50 μg/mL, the contrast ratio approaches 1.9, which indicates that there is some preferential binding of the antigen/antibody complex (via a second antigen binding site on the antibody) to TNP-containing regions on the polymer. Since the degree of nonspecific binding remained constant over the concentration range of 2,4-DNP employed, the contrast ratio was mainly determined by the amount of specific binding. It is worth noting in Figure 7 that the errors in measurement are smaller at the lower 2,4-DNP concentrations because the Gaussian distribution of pixel intensities in the histogram (See Experimental Section) was smaller when the integrated areas were brighter (higher fluorescence ratios). We are currently in the process of determining the MDC of 2,4-DNP which can be measured using these antigen-patterned substrates in a competition immunoassay format.

Experimental Section

Chemicals and Materials. Allyl isocyanate (Aldrich, 98%), Bio-Gel P-10 gel medium (Bio-Rad), 2,6-dinitrobenzaldehyde (Aldrich, 99%), 2,4-dinitrophenol (Aldrich), fluorescamine (Fluka), iodination reagent kit (IODO-BEADS) (Pierce), 3-methacryloxypropyltrimethoxysilane (MPTS) (Hüls America), $Na^{125}I$ (NEN/DuPont), 2-nitrobenzyl alcohol (Fluka), phosphate-buffered saline (NaCl, 120 mM; KCl, 2.7 mM; monobasic and dibasic phosphate buffer salts, 10 mM; pH 7.4) (PBS) (Sigma), potassium persulfate (Bio-Rad), ScintiVerse II (Fisher), Sephadex G-25 (Sigma), *N,N,N′,N′*-tetramethylethylenediamine (TEMED) (Bio-Rad), anti-dinitrophenyl, rabbit IgG (H + L) fraction, tetramethylrhodamine conjugate (α-DNP-TRITC-IgG) (Molecular Probes), 2,4,6-trinitrobenzenesulfonic acid (TNBSA) (Pierce), Triton X-405 (Aldrich), and *p*-xylene (HPLC grade, Aldrich) were all used as received. Acrylamide (Bio-Rad 99.9%) was twice recrystallized from chloroform and stored under argon in the dark at −80 °C. *N,N′*-Methylenebisacrylamide (bis-acrylamide) (Bio-Rad, 99.9%) was recrystallized from acetone. 2,6-Dinitrophenylmethanol was prepared by the method of Houlihan *et al.*[56] Polished native Si wafers (⟨100⟩, P-doped, n-type, min resistivity 5.000 Ω cm) (MEMC Inc.) were cleaned as described below. Fused silica slides (2.54 × 2.54 × 0.1 cm) (Dell Optics) and microscope cover slips (borosilicate, 11 × 22 mm, #2, Thomas Scientific) were cleaned (vide infra) prior to use. Mylar strips (4 μm thickness) (Kinmar Polyester) were used as spacers. Polymer solutions were filtered using Acrodisc 3 CR poly(tetrafluoroethylene) (PTFE) (0.45 μm) filters (Gelman). Water with resistivity > 18 MΩ cm was used in all experiments.

Preparation of 2-Nitrobenzyl *N*-Allylcarbamate (2-NBAC) (1). To a solution of 2-nitrophenylmethanol (7.0 g, 46 mmol) in anhydrous tetrahydrofuran (70 mL) under argon was added an ethereal solution of methyllithium (1.42 M, 3.25 mL, 4.60 mmol). The resulting solution was stirred for 2 h and then treated dropwise with a solution of allyl isocyanate (4.1 mL, 3.9 g, 46 mmol) in anhydrous tetrahydrofuran (45 mL). Once the addition was complete, the solution was stirred for 30 min and concentrated in vacuo. The residue was taken up in ether (300 mL) and washed with water (3 × 200 mL) and brine (1 × 200 mL). After drying ($MgSO_4$), the solvent was removed under reduced pressure to give a crude light yellow solid (9.24 g). The pure product was isolated by extraction with hot hexane (3 × 50 mL). After cooling to 4 °C for 12 h, the desired carbamate (**1**) crystallized as long white needles (7.56 g, 70%), mp 59−61 °C. Anal. Calcd. for $C_{11}H_{12}N_2O_4$ (236.23): C, 55.93; H, 5.12; N, 11.86. Found: C, 55.84; H, 5.01; N, 11.73. IR (cm^{-1}, KBr): 3314 (s, N-*H* str), 1697 (s, C═O str), 1521 (s, asymm N−O str), 1341 (m, symm N−O str). ^1H NMR (ppm, $CDCl_3$): δ 3.83 (2 H, t, RCHCH_2NHR), 4.85−5.10 (1 H, br s, −NH−), 5.13−5.25 (2 H, complex m, CH_2═CHR), 5.53 (2 H, s, CH_2OCOR), 5.78−5.93 (1 H, complex m, CH_2═C*H*R), 7.47 (1 H, dt, $J_o = 8$ Hz, $J_m = 2$ Hz, H *para* to NO_2), 7.62 (2 H, overlapping dd, *meta* to NO_2), 8.09 (1H, d, $J_o = 8$ Hz, H *ortho* to NO_2). ^{13}C NMR (ppm, $CDCl_3$): δ 43.46 (RCH*C*H_2NHR), 63.23 (H_2*C*OCOR), 116.20 (*C*H_2═CHR), 124.87 (C *ortho* to NO_2), 128.47 (C *ortho* to CH_2OCOR), 128.64 (C *para* to CH_2OCOR), 133.09 (C *para* to NO_2), 133.68 (CH_2═*C*HR), 147.27 (C *ipso* to NO_2), 155.62 (CH_2O*C*OR). λ_{max}^{MeOH} 258 nm [log ϵ (3.84 ± 0.02)].

(56) Houlihan, F. M.; Shugard, A.; Gooden, R.; Reichmanis, E. *Macromolecules* **1988**, *21*, 2001.

Preparation of 2,6-Dinitrobenzyl *N*-Allylcarbamate (2,6-DNBAC) (2). To a solution of 2,6-dinitrobenzenemethanol[57] (2.01 g, 10.1 mmol) in anhydrous tetrahydrofuran (15 mL) under argon was added an ethereal solution of methyllithium (1.42 M, 0.72 mL, 1.02 mmol). The resulting solution was stirred for 2.5 h and then treated dropwise with a solution of allyl isocyanate (0.90 mL, 0.85 g, 10.2 mmol) in dry tetrahydrofuran (10 mL). Once the addition was complete, the solution was stirred for 30 min and concentrated in vacuo. The residue was taken up in ether (150 mL) and washed with water (3 × 25 mL) and brine (1 × 25 mL). After drying ($MgSO_4$), the solvent was removed under reduced pressure to give a brown solid (2.86 g), which after flash chromatography on silica gel (dichloromethane) afforded the desired carbamate (**2**) as a light yellow solid (1.76 g, 62%), mp 99−100 °C. Anal. Calcd for $C_{11}H_{11}N_3O_6$ (281.06): C, 46.96; H, 3.94; N, 14.95. Found: C, 46.91; H, 3.55; N, 14.91. IR (cm^{-1}, KBr): 3409 (s, N−H str), 1719 (s, C═O str), 1530 (s, asymm N−O str), 1368 (m, symm N−O str). ^{1}H NMR (ppm, $CDCl_3$): δ 3.72 (2 H, t, RCHCH_2NHR), 4.77−4.90 (1 H, br s, −N*H*−), 5.05−5.20 (2 H, complex m, CH_2═CHR), 5.53 (2 H, s, CH_2OCOR), 5.65−5.85 (1 H, complex m, CH_2═C*H*R), 7.65 (1 H, t, J_o = 8 Hz, H *meta* to NO_2), 8.01 (2 H, d, J_o = 8 Hz, H *ortho* to NO_2). ^{13}C NMR (ppm, $CDCl_3$): δ 43.32 (RCH*C*H_2NHR), 58.37 (H_2COCOR), 116.18 (*C*H_2═CHR), 126.70 (C *ipso* to CH_2OCOR), 127.67 (C *para* to CH_2OCOR), 129.77 (C *meta* to CH_2-OCOR), 133.75 (CH_2═*C*HR), 150.77 (C *ipso* to NO_2), 154.90 (CH_2OCOR). λ_{max}^{MeOH} 230 nm [log ϵ (4.14 ± 0.02)].

Solution Photolysis Kinetics. The solution photolyses of **1** and **2** in dry acetonitrile or acetonitrile-d_3 were monitored by reversed-phase liquid chromatography (RPLC), gas chromatography/mass spectrometry (GC/MS), thermospray/high-performance liquid chromatography/mass spectrometry (TSP/HPLC/MS), and ^{1}H NMR spectroscopy. Samples were prepared in the following manner: to 2.0 mL of dry, degassed acetonitrile in a quartz cuvette was added 10 mg of carbamate. To this solution was added 40 μL of *p*-xylene to serve as an internal chromatography standard. Samples were irradiated (220 nm, 10.5 mW cm^{-2}) for successive 3-min intervals after which 25 μL of the photolyzed solution was withdrawn and prepared for RPLC by adding 350 μL of acetonitrile and 650 μL of water. A 25-μL injection was made onto the column and absorbance monitored at 230 nm. The progress of photochemical rearrangement was followed by monitoring the decrease in integrated area of the starting carbamate in relation to the integrated area of *p*-xylene. The percent nitrobenzyl carbamate remaining was calculated by use of the following equation:

$$\%\ \text{carbamate remaining} = \frac{\text{final (area carbamate/area } p\text{-xylene)}}{\text{initial (area carbamate/area } p\text{-xylene)}} \times 100 \quad (3)$$

The percent conversion due to each exposure was found by subtraction (eq 4):

$$\%\ \text{conversion of carbamate} = 100 - \%\ \text{carbamate remaining} \quad (4)$$

Solid-State Photolysis Kinetics. Solid-state photochemical studies were performed using dispersions of **1** and **2** in KBr pellets. A well-ground mixture of KBr (125 mg) and carbamate (0.3 mg) was pressed into a pellet (13 mm diameter, 0.4 mm thickness) at 4500 psi. All disks used were optically transparent in the visible region of the spectrum. Irradiation was performed using the same source and lamp output as in the solution-phase experiments described above. The photochemical rearrangement was followed by monitoring the disappearance of the N−H stretch at 3314 cm^{-1} for **1** and at 3409 cm^{-1} for **2** in relation to the aromatic C−H out-of-plane bending bands at 731 cm^{-1} for **1** and at 760 cm^{-1} for **2**, which were used as the reference bands. The ratio (area NH_2 band/area C−H bending band) was calculated initially and then again after each successive UV exposure dose. Samples were irradiated (220 nm, 10.5 mW cm^{-2}) for successive time intervals after which the IR spectrum was recorded. The percent nitrobenzyl carbamate remaining after exposure was calculated by use of the following equation:

$$\%\ \text{carbamate remaining} = \frac{\text{final (area NH}_2\text{ band/area C−H bending band)}}{\text{initial (area NH}_2\text{ band/area C−H bending band)}} \times 100 \quad (5)$$

The percent conversion due to each exposure was found by subtraction (eq 4).

Substrate Cleaning and Silane Deposition. Fused silica slides, microscope cover slips, and Si wafers were cleaned by rubbing with methanol-soaked wipes followed by sonication in water for 30 s. After rinsing with water, they were submerged in 1 M KOH for 30 min at 60 °C. The substrates were rinsed with water and transferred to a solution of HCl/methanol (1:1) where they were sonicated for 1 min and then heated for 30 min at 60 °C. After a final rinse with water, they were dried in a jet of nitrogen. They were divided into two groups of equal number. Group 1 was immersed for 1 h in a solution of dichlorodimethylsilane (1%, v/v, in hexane), rinsed with hexane, dried in a jet of nitrogen, and baked at 120 °C for 5 min. Group 2 was treated for 1 h at 60 °C in a solution containing methanol (193 mL), water (5.4 mL), glacial acetic acid (0.6 mL), and MPTS (1.0 mL). They were then rinsed in methanol, dried in a jet of nitrogen, and baked at 120 °C for 5 min.

Polymerization and Deposition. To 1.0 mL of water was added acrylamide (0.36 g, 5.1 mmol), bisacrylamide (0.040 g, 0.26 mmol), and 2,6-dinitrobenzyl *N*-allylcarbamate (**2**) (3.0 mg, 0.011 mmol). The resulting mixture was sonicated at 60 °C until all solids dissolved. After cooling to room temperature, the solution was deoxygenated by sparging with argon for 5 min. Potassium persulfate (2.0 mg, 7.4 μmol) was added, and the solution was passed through a 0.45-μm filter. The catalyst, TEMED (3.0 μL, 20 μmol), was added, and the mixture was briefly stirred. Within 1 min of the TEMED addition, 20 μL of the solution was applied to the surface of the MPTS-modified substrate, which was immediately covered with a second substrate that had been modified with dichlorodimethylsilane. The resulting "sandwich" (produced using a variation of the flap

(57) Neenan, T. X.; Houlihan, F. M.; Reichmanis, E.; Kometani, J. M.; Bachman, B. J.; Thompson, L. F. *Macromolecules* **1990**, *23*, 145.

technique)[48] was clamped together with binder clips and was allowed to polymerize under a nitrogen atmosphere for 12 h at room temperature. After the substrates were separated, the MPTS-modified substrate containing the polymer film was soaked in water for 15 min, sonicated for 10 s, and dried in a jet of nitrogen.

Polymerization Kinetics. An argon-saturated solution of monomer, cross-linker, catalyst, initiator, and **2** was prepared as above and quickly transferred to a 1-mm cuvette using a gastight syringe. Absorbance readings were taken at 283 nm at 2-min intervals for a total reaction time of 100 min. Catalyst addition, cuvette positioning, and initiation of data collection took less than 30 s. An aqueous solution of catalyst and initiator at the appropriate concentrations was used in the reference cell. The polymerization reaction was judged complete when the change in absorbance at 283 nm was less than 0.0025 AU/min.

Photoactivation and Characterization of Polyacrylamide Films. Samples were prepared by depositing 1.0 ± 0.2 μm films (as measured by profilometry) on quartered Si wafers or fused silica slides using the method described above. They were irradiated (10.5 mW cm^{-2} at 220 nm) for increasing time intervals. Photoconversion was monitored using IR spectroscopy, fluorescence imaging, and UV−visible spectroscopy (after reaction with amine-specific color reagents).

For IR experiments, samples were allowed to equilibrate in the nitrogen-purged sample compartment for 10 min prior to scanning. An MPTS-modified Si wafer was used for the background spectrum. All spectra were acquired in transmission mode using 128 scans and a resolution of 4 cm^{-1}. In fluorescence experiments, polymer-modified slides were irradiated for increasing time intervals (0−30 min), immersed in a solution of fluorescamine (25 mg/L in acetone with 0.5% triethylamine) for 30 min, rinsed with acetone, and dried in air. The fluorescence spectrum of each substrate was then measured (390-nm excitation, 475-nm emission). Irradiated films were also treated for 30 min with a filtered (0.22 μm) solution of TNBSA (1 g/L in 0.1 M borate buffer, pH 8.5). They were then rinsed with copious amounts of borate buffer, rinsed and soaked for 5 min in PBS/Triton X-405 [(1×10^4):1], and rinsed and soaked for 5 min in water. After the films were dried in a jet of nitrogen, the UV−visible spectrum was recorded. Absorbance due to trinitrophenyl (TNP) amino groups was measured at 420 nm (extinction coefficient, 19 200 M^{-1} cm^{-1}).[51] Absorbance values obtained were corrected for variations in polymer film thickness. TNBSA labeling experiments were performed in triplicate.

Production of Antigen and Antibody-Patterned Substrates. A metallized quartz line-space mask (5-μm lines, 10-μm spaces) was used to selectively irradiate regions of a polymer-coated fused silica slide for 10 min (6.3 J cm^{-2} dose at 220 nm). The polymer was reacted with TNBS as described in the preceding section. This antigen-modified substrate was exposed to a solution of anti-dinitrophenyl rabbit IgG (H + L) fraction, tetramethylrhodamine conjugate (α-DNP-TRITC-IgG) (10 μg/mL in PBS), for 30 min. It was rinsed with PBS and water prior to examination with a laser scanning confocal fluorescence microscope (LSCFM). The substrate was imaged in air using an excitation wavelength of 514 nm and measuring the emission at wavelengths above 565 nm.

Preparation of ^{125}I-Radiolabeled Antibodies. α-DNP-TRITC-IgG was labeled with ^{125}I using the *N*-chlorobenzenesulfonamide method[58] and an iodination reagent kit (IODO-BEADS). For our experiments, 0.8 μCi of Na^{125}I was added to 600 μL of α-DNP-TRITC-IgG (1.6 mg/mL in PBS). One IODO-BEAD was added to the solution, which was then gently agitated for 30 min. The bead was then removed, and the radiolabeled protein was passed through a gel filtration column of Sephadex G-25 using PBS as the mobile phase. The ^{125}I-labeled protein (specific radioactivity, 2.3 μCi/mg of protein) was collected, stored at 4 °C, and used within 1 week. The concentration of iodinated protein was determined by measuring the UV absorbance of the protein solution at 278 nm using $\epsilon_{278\text{nm}}{}^{0.1\%} = 1.35$.

Determination of Antibody Surface Concentration. Two sets of samples were used in ^{125}I-labeling experiments. In the first samples, polyacrylamide containing 2,6-DNBAC (DNBAC−PA) was deposited on microscope cover slips, irradiated for 30 min, and reacted with TNBSA to produce antigen-modified substrates as described above. The second set of samples consisted of DNBAC−PA substrates that were not exposed to light or TNBSA. Both sets were immersed in a solution of α-DNP-TRITC-IgG (10 μg/mL) containing a sufficient quantity of [^{125}I]α-DNP-TRITC-IgG to produce a solution with a specific activity of approximately 1000 cpm/μg of protein. The solutions were agitated for 30 min using a shaker plate at 50 rpm. The substrates were then thoroughly rinsed with PBS, PBS/Triton X-405 [(1×10^4):1], and water. Each cover glass was placed into a separate vial with 10 mL of scintillation fluid (ScintiVerse II) and counted five times. All experiments were performed in quadruplicate, and the average value was used to calculate antibody surface concentrations.

Competition Immunoassay Using Patterned Substrates. Antigen analogue (TNP) patterned substrates (described above) were treated for 30 min with solutions of α-DNP-TRITC-IgG (10 μg/mL in PBS) containing varying amounts of 2,4-DNP. The substrates were then thoroughly rinsed with PBS, PBS/Triton X-405 [(1×10^4):1] and water. After drying in air, they were imaged using a LSCFM. All 8-bit image data files were exported into Image-Pro software, and a histogram of the pixel value distribution was constructed. The resulting bimodal distribution (representing dark and light regions of the image) was fit to a two-peak Gaussian equation to determine the peak centers and associated standard deviations. The fluorescence contrast ratio is defined as $x1_0$: $x2_0$ where $x1_0$ = center of peak 1 (distribution of pixel intensities representing bright regions), and $x2_0$ = center of peak 2 (distribution of pixel intensities representing dark regions). The experiment was performed in triplicate, and the intensity ratios were reported as the mean ± SD for each 2,4-DNP concentration employed.

Instrumentation. Melting points were determined using a capillary melting point apparatus (MEL-TEMP

(58) Markwell, M. A. K. *Anal. Biochem.* **1996**, *125*, 427.

II, Laboratory Devices) and are reported uncorrected. Infrared spectra were obtained using an FT IR spectrometer (Magna-IR 750, Nicolet). Ultraviolet−visible spectra were measured using a spectrophotometer (Cary 2400, Varian). NMR spectra were recorded using a 250-MHz spectrometer (AC 250, Bruker). Microanalyses were performed by Oneida Research Services, Inc., Whitesboro, NY. Thermospray/HPLC/MS was performed by Oneida Research Services, Inc., using the following instruments and conditions: (1) an HPLC system (600MS, Waters) with a reversed-phase column (LC-8-DB, 0.46 × 15 cm, Supelco) using a linear gradient between water and acetonitrile, (2) a postcolumn buffer (50 mM ammonium acetate) at a flow rate of 0.3 mL/min, and (3) a mass spectrometer (TSQ-70 with TSP2 interface, Finnigan) scanning *m*/*z* 150−550 at 1.5 s/scan. Thermal desorption chemical ionization mass spectra were obtained in positive and negative ion mode using a triple quadrapole mass spectrometer (TSQ-70, Finnigan) with methane serving as the reagent gas. Chromatography was performed using an HPLC system (2010 Millennium, Waters) consisting of two pumps (model 510, Waters), an injector (model U6K, Waters), and a photodiode-array detector (model 996, Waters). A reversed-phase column (Nova-Pak C_8, 8 × 100 mm, Waters) with a linear gradient (flow rate, 1.5 mL/min) between water and acetonitrile was used in all experiments. Solution and solid-state photolyses were performed using an illuminator (model 87435, Oriel) equipped with a 500-W mercury(xenon) lamp filtered by a dichroic mirror to give a source spectrum of 220−260 nm. Exposure times were controlled by a timer−integrator (model 84360, Oriel). Light intensities were measured using an optical power meter with a 220/253.7-nm probe (model 100, Mimir Instruments). Fluorescence micrographs were obtained using a LSCFM (Sarastro 2000, Molecular Dynamics) equipped with ImageSpace software (Molecular Dynamics). Fluorescence emission spectra were measured using an SLM/AMINCO 8000 fluorimeter (SLM Instruments). Film thickness was measured using a profilometer (Dektak, Sloan Technology). Radioactivity was measured with a liquid scintillation analyzer (TRI−CARB 1500, Packard).

Acknowledgment. The authors would like to thank Barry Spargo for his assistance with the LSCFM. We thank John Callahan for performing the thermal desorption chemical ionization mass spectroscopy. John Bart and Anna Davis are also to be thanked for their many helpful discussions and invaluable assistance in preparing the manuscript. This work was supported by the Office of Naval Research (ONR) and the Defense Advanced Research Projects Agency (DARPA).

CM970632T